Melt Spinning of High-Impact Polystyrene: Rubber Morphology Variations, Orientation Development, and Mechanical Properties

M. A. A. OMOTOSO, JAMES L. WHITE, and JOHN F. FELLERS, *Polymer Engineering Department, University of Tennessee, Knoxville, Tennessee 37916*

Synopsis

Studies of melt-spun, high-impact polystyrene filaments indicate that rubber globules are fragmented to smaller sizes with increasing drawdown ratio and spinline stress. The melt-spun fibers are highly birefringent and obey the same relationship between birefringence and stress as pure polystyrene despite the presence of the rubber globules. These results are interpreted in terms of the stress distribution across the filament cross section. Room temperature tensile force–elongation curves were obtained on the filaments, and mechanical property phenomena were interpreted in terms of the above morphology changes and orientation of polystyrene chains.

INTRODUCTION

Most attention to structural changes during solidification, i.e., vitrification, of commercial polystyrenes has been paid to the unmodified pure glassy polystyrene.[1–19] These studies have dealt with the development of orientation and thermal stresses during solidification under mechanical stress and in processing. There have been few studies of this type for high-impact polystyrene (HIPS), probably because of the extensive scattering of light (and depolarization associated with scattering) by the rubber globules (see the comments of Wales, van Leeuwen, and van der Vigh[12]). Thomas and Cleereman[20] have described the development of orientation in biaxially stretched sheets of HIPS and characteristics of the rubber morphology. Thomas and Cleereman[20] report two micrographs showing how the biaxial stretching process influences the rubber morphology of HIPS. Grancio and co-workers[21,22] have investigated this problem in cold rolling and hot stretching of ABS resins. Thamm[23] has studied the influence of injection molding on rubber morphology of rubber-modified polypropylene.

It is the purpose of this article to present an experimental study of the development of orientation and variations in rubber morphology occurring during the melt spinning of HIPS and to investigate their influence on the mechanical properties of the fibers formed. This study represents a continuation of the authors investigations of (1) the development of orientation in vitrifying glasses by melt processing,[15,24] (2) mechanical properties of glasses,[25,26] and (3) structure development in melt spinning.[15,24,27–32]

Journal of Applied Polymer Science, Vol. 25, 1573–1585 (1980)

0021-8995/80/0025-1573$01.30

EXPERIMENTAL

Materials. A series of commercial and experimental rubber-modified polystyrenes supplied by Dow and Union Carbide were used in this study. These polymers are summarized in Table I.

Melt Spinning. The polymers were brought into the molten state and extruded at 180°C from an Instron capillary rheometer. A die with diameter of 0.058 in. and length-to-diameter ratio of 17 was used to extrude the filaments. They were taken up with a variable speed control Bodine electric motor at velocities V_L of 2–30 m/min. Drawdown ratios V_L/V_0 of 5–35 were used. The fibers were spun directly into an ice water bath.

Morphology. The rubber phase morphology in the melt-spun fibers was studied using a Philips EM 300 100 kV transmission electron microscope (TEM). The samples were prepared by first staining the filaments with a 1% solution of osmium tetroxide for 2 hr. In some cases the samples were embedded in an epoxy resin for microtoming done with an LKB Ultratome (III) utramicrotone. Samples were also prepared by film casting from a 1% benzene solution onto a copper grid. Fracture surfaces made from samples broken in liquid nitrogen were investigated using an AMR model 900 scanning electron microscope (SEM).

Birefringence. The birefringence was determined using Olympic and Leitz polarizing light microscopes with fibers placed between crossed polars. Berek-type compensators were used to determine retardation.

Mechanical Properties. The room temperature mechanical properties of the filaments were determined using a table model Instron tensile tester. The initial gauge length was 2 cm and the sample was elongated at a rate of 2 cm/min. The tensile strength was derived from the force at fracture and the original cross-sectional area A_0. The Young's modulus E was defined as

$$E = \lim_{\gamma \to 0} \frac{\Delta\sigma}{\Delta\gamma} \tag{1}$$

where σ is the engineering stress (F/A_0) and γ is the infinitesimal strain. The Young's modulus, tensile strength, yield stress, and elongation at break were averages of three repeat experiments.

TABLE I
HIPS Samples Investigated in this Study

Designation	Rubber content, %	Supplier
B	7	Union Carbide
C	10	Union Carbide
D	13.5	Union Carbide
E	5	Dow Styron 430U
F	7	Dow Styron 470U
G	10	Dow Styron 492U
H	12–15	Dow Styron 495

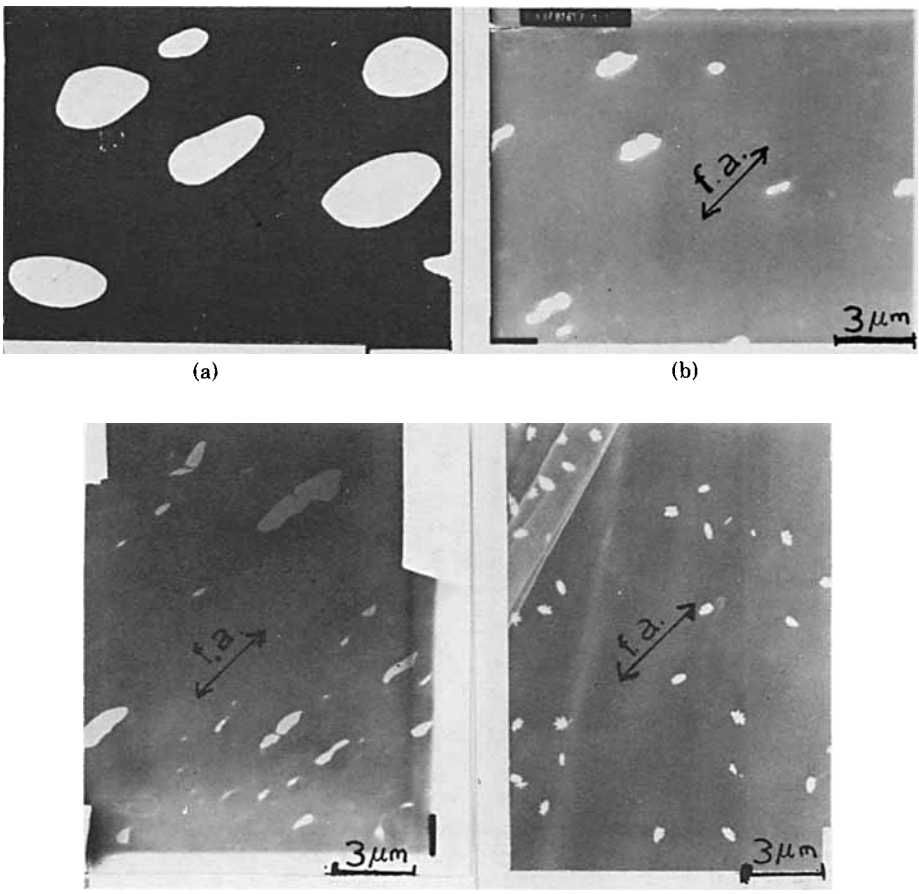

Fig. 1. TEM photomicrographs of melt-spun fibers of sample HIPS E as a function of spinning conditions (drawdown ratio, spinline stress).

RUBBER MORPHOLOGY

Results

TEM photomicrographs were made on samples B and F as a function of spinning conditions. The specimens for TEM observation were prepared by either microtoming or solvent casting. The former was used on both samples and the latter on E. Typical micrographs are shown in Figures 1 and 2. Clearly, increasing drawdown or stress makes the rubber particles become smaller and smaller. The rubber particles become ellipsoidal in shape with the major axis of the ellipsoid being parallel to the fiber axis. If the major axis has length b and the minor axis a, the equivalent diameter is

$$d = \sqrt[3]{ba^2} \tag{2}$$

Number average d_n and weight average d_w diameters of rubber particles were determined from the expressions

$$d_n = \sum N_i d_i / \sum N_i, \quad d_w = \sum N_i d_i^2 / \sum N_i d_i \tag{3}$$

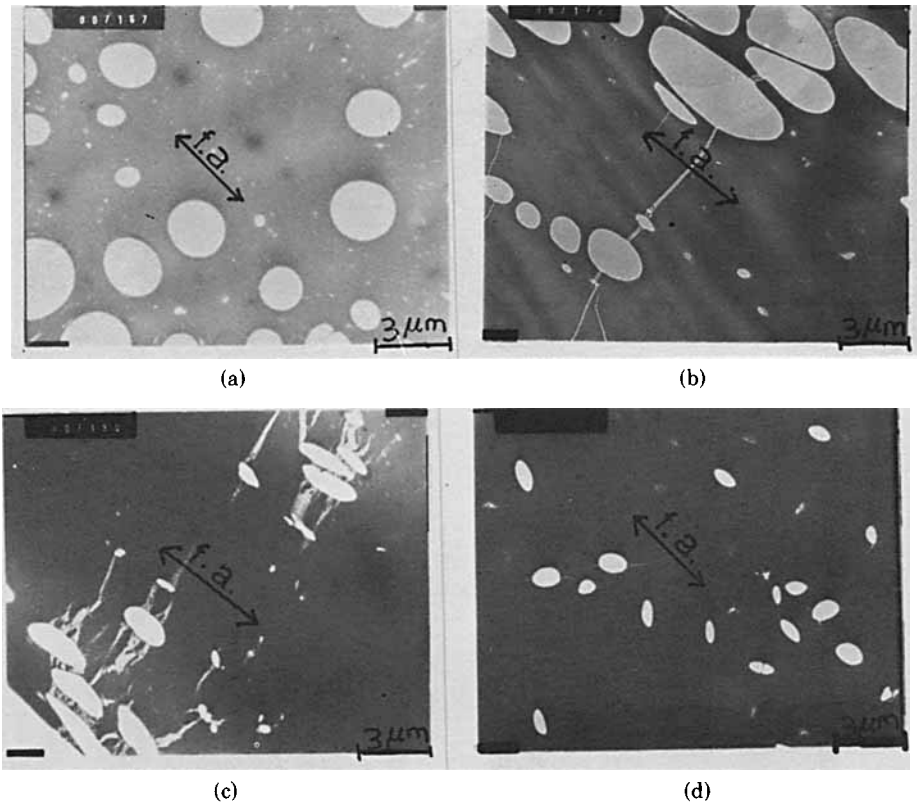

Fig. 2. TEM photomicrographs of melt-spun fibers of sample HIPS B as a function of spinning conditions (drawdown ratio, spinline stress); f.a. denotes fiber axis.

where N_i is the number of particles of diameter d_i. Sample sizes of 6–30 globules were used for the initial B sample. The initial values of d_n and d_w/d_n were 2.3 μm and 1.7. In the fibers spun under the most severe conditions, these became 0.8 μm and 1.1. For sample E, initial values of 2.0 μm and 1.1 were changed to 0.23 μm and 1.0 with drawdown. The variation of d_n with spinning conditions is shown in Figure 3.

SEM fracture surfaces for the filaments are shown in Figure 4. These were also used to determine rubber particle sizes.

In Table II, we summarize values of d_n and d_w obtained from TEM and SEM data as a function of spinline drawdown and stress.

Discussion

It would appear that the rubber globules are reduced in size in the melt spinning process by tensile fracture of the rubber globules. This continues to occur with increasing drawdown and spinline stress. The tensile strength of lightly crosslinked elastomers is about 10^8 dyn/cm^2 at room temperature and reduces to about 2% of this value (2×10^6 dyn/cm^2) at 120°C. It can be seen from Table II that the spinline stresses equal or exceed this value. If the stresses apply uniformly over the cross section and on rubber globules as well as melt, stresses greater than the tensile strength of the rubber will be acting.

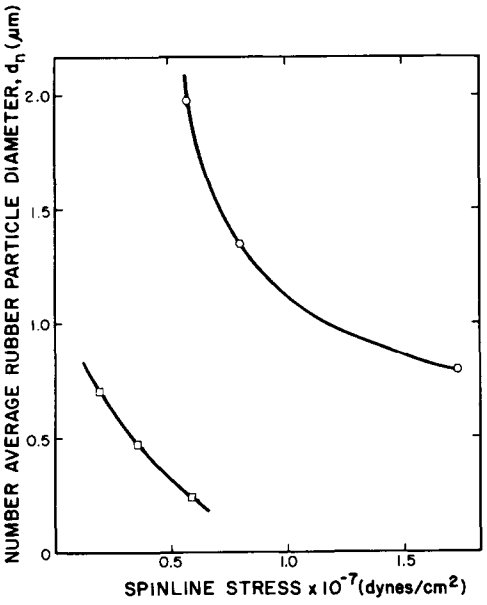

Fig. 3. Number-average rubber particle diameter d_η as a function of spinline stress for (○) sample B, and (□) sample E.

TABLE II
Rubber Particle Sizes in HIPS

Sample	Drawdown ratio	Spinline stress ($\times 10^{-6}$ dyn/cm^2)	TEM Particle sizes (μm) d_n (μm)	TEM Particle sizes (μm) d_w (μm)	TEM Particle sizes (μm) d_w/d_n	SEM Particle sizes (μm) d_n (μm)	SEM Particle sizes (μm) d_w (μm)	SEM Particle sizes (μm) d_w/d_n
B	(virgin sample)		2.31	3.89	1.68	1.90	2.20	1.16
	11.1	1.9	1.97	2.79	1.42	1.39	1.66	1.2
	19.2	3.7	1.36	1.68	1.24	1.02	1.20	1.18
	27.6	5.9	0.80	0.90	1.10	0.50	0.53	1.06
E	(virgin sample)		1.96	2.16	1.10			
	11.1	5.7	0.69	0.85	1.24			
	19.2	7.9	0.56	0.62	1.10			
	24.9	17.5	0.23	0.23	1.0			

We should explore the above ideas further. Generally stresses are not applied uniformly to different phases in a cross section, but are preferentially applied to regions of higher modulus. We may write

$$F_{\text{HIPS}} = \bar{\sigma}A = \int_0^{A_{\text{PS}}} \sigma_{\text{PS}} dA_{\text{PS}} + \int_0^{A_R} \sigma_{\text{R}} dA_{\text{R}} \tag{4}$$

$$A = A_{\text{PS}} + A_{\text{R}}$$

where F_{HIPS} is the total spinline force, $\bar{\sigma}$ is the mean stress, σ_{PS} is the polystyrene stress field, and σ_R is the rubber globule stress field.

The stress distribution for the two phases may be approximately described if the strain is small and equal in both phases. A Takayangi parallel model would approximate the behavior with

$$\sigma_{\text{PS}} = E_{\text{PS}}\gamma_{\text{PS}} \tag{5a}$$

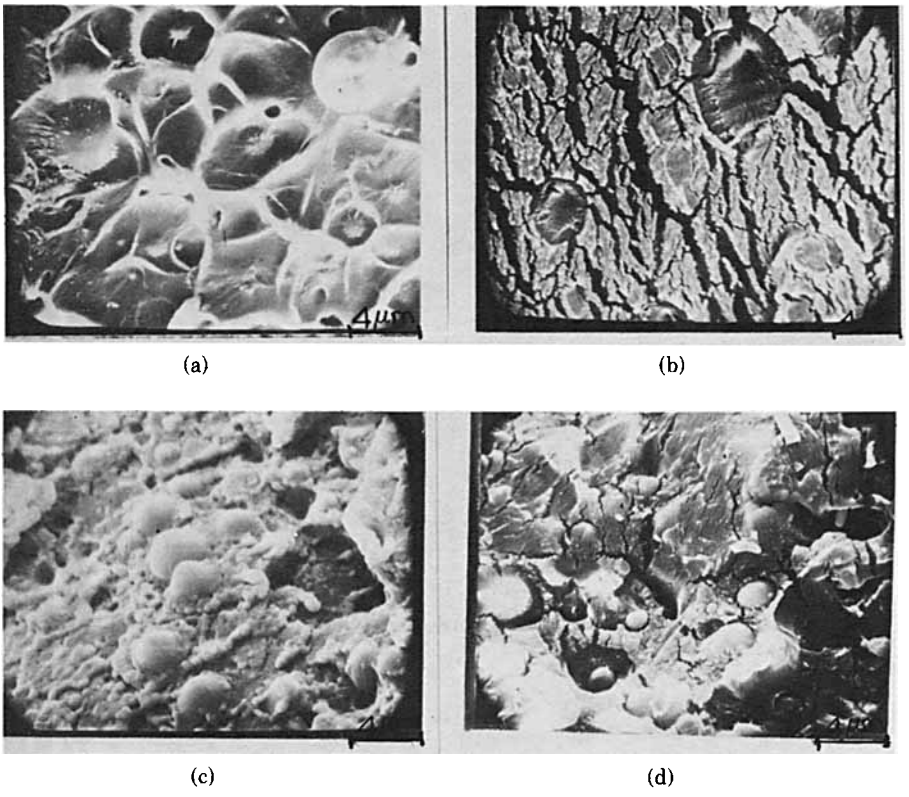

Fig. 4. SEM fracture surfaces of melt-spun HIPS samples.

$$\sigma_R = E_R\gamma_R \tag{5b}$$

$$\gamma_R = \gamma_{PS} = \gamma \tag{5c}$$

$$F_{HIPS} = (A_{PS}E_{PS} + A_RE_R)\gamma \tag{5d}$$

and

$$\sigma_R = (E_R/E_{PS})\sigma_{PS} \tag{6}$$

At low temperatures where E_{PS} is much greater than E_R, the polystyrene phase takes up most of the stress. However, at temperatures above T_g, the modulus E_{PS} is substantially reduced and the stresses on the rubber phase elevated. As the polystyrene is a viscous melt and the rubber, apparently, a lightly crosslinked elastomeric phase, the relative stresses imposed on the later phase will increase further as the temperature rises. Above T_g, σ_R must be greater than σ_{PS}.

Similar arguments can be developed if we presume that both phases behave as viscoelastic fluids with elongational viscosity χ. The elongation rate $\dot{\gamma}$ must be the same in both phases

$$\sigma_{PS} = \chi_{PS}\dot{\gamma}_{PS} \tag{7a}$$

$$\sigma_R = \chi_R\dot{\gamma}_R \tag{7b}$$

$$\dot{\gamma} = \dot{\gamma}_{PS} = \dot{\gamma}_R \tag{7c}$$

$$F_{HIPS} = (A_{PS}\chi_{PS} + A_R\chi_R)\dot{\gamma} \tag{7d}$$

and

$$\sigma_R = [\chi_R(T,\dot{\gamma},t)/\chi_{PS}(T,\dot{\gamma},t)]\sigma_{PS} \tag{8}$$

As the rubber phase is a lightly crosslinked solid χ_R will presumably go to infinity at finite strains again making σ_R greater than σ_{PS}.

OPTICAL AND BIREFRINGENT CHARACTER

Results

The fibers become increasingly transparent as the drawdown level increases.

In Figure 5 we plot the birefringence of selected HIPS as a function of take-up velocity. The birefringence is found to be *negative,* i.e., $n_1 < n_2$, and is in the range of 10^{-3} to 10^{-2}. Birefringence increases with increasing drawdown of the filaments. The level of birefringence however varies from sample to sample.

We replot the data-versus-spinline stress in Figure 5. A better correlation is found. It is also a linear dependence. The birefringence–stress relation may be written

$$\Delta n = C\sigma_{11} = C(F/\pi R^2) \tag{9}$$

where C is an apparent stress-optical constant and corresponds to a value of C of -4500 Brewster (B) (1 B = 10^{-13} cm^2/dyn).

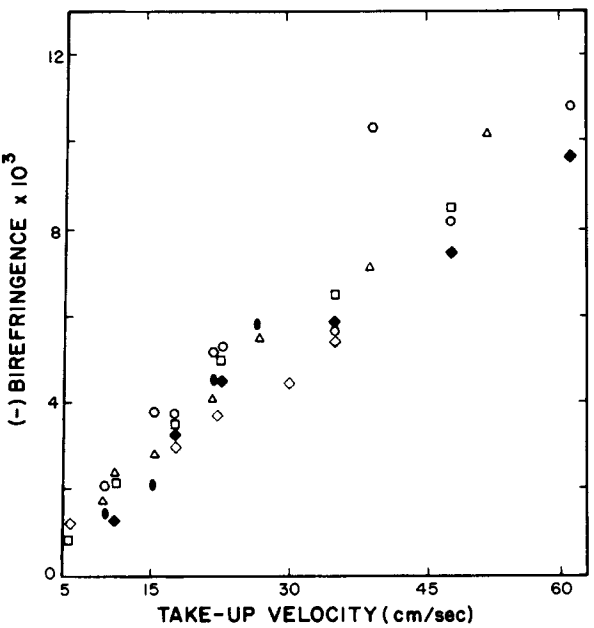

Fig. 5. Birefringence of melt-spun HIPS fibers as a function of take-up velocity for samples (○) B, (△) C, (●) D, (□) E, (⊙) F, (♦) G, (◇) H.

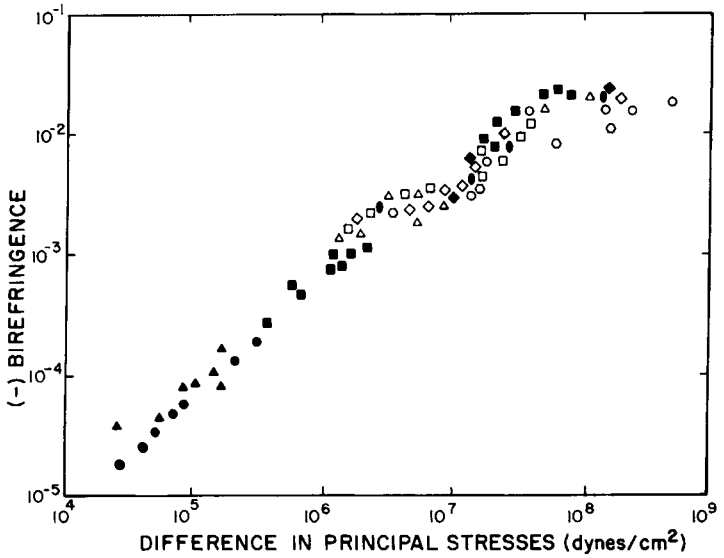

Fig. 6. Birefringence of HIPS [(○) B, (△) C, (●) D, (□) E, (○) F, (♦) G, (◇) H] and PS [(■) melt spun, (●) elongational flow, (▲) simple shear] samples (Oda et al.) as a function of difference in principal stresses. The open points are HIPS samples. The closed points are PS samples of Oda et al.

Discussion: Birefringence of Different Phases

The increasing transparency of the filaments would appear in some part to be due to the decreasing size of the rubber globules.

The HIPS Δn–σ data appear similar in character to the correlation developed by Oda, White, and Clark[15] for melt-spun polystyrene filaments. We plot their data together with ours in Figure 6. The agreement between our results and those of Oda et al. are excellent and correspond to a stress-optical constant of −4500 B. It would appear that the rubber does not play an important role. This result was suggested to us independently by M. Fleissner (Hoechst AG).

HIPS is a two-phase system and its birefringence should be a complex function of the birefringence in the individual phases and form birefringence

$$\Delta n = (1 - \phi)\Delta n_{PS} + \phi\Delta n_{R} + \Delta n_{form} \quad (10)$$

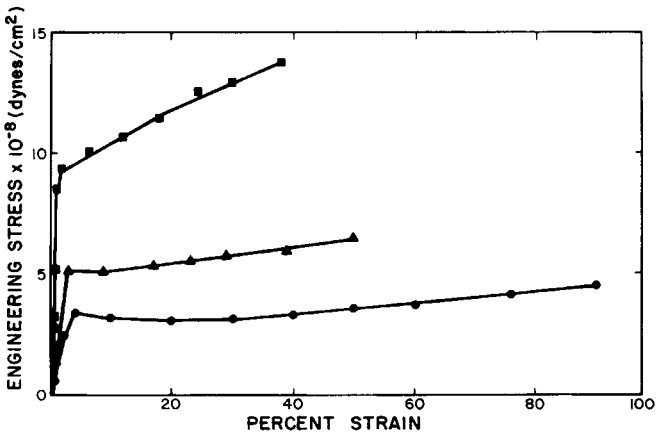

Fig. 7. Engineering stress–strain curves for melt-spun fibers [spinline stress (dyn/cm²): (●) 0.5 × 10⁷, (▲) 2.0 × 10⁷, (■) 5.0 × 10⁷].

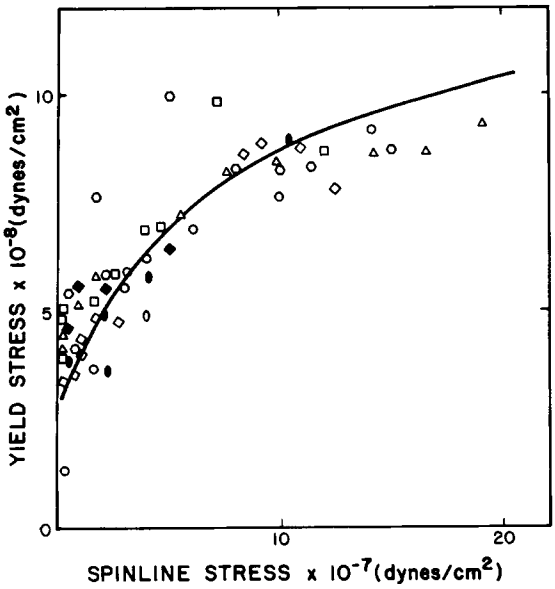

Fig. 8. Yield stress as a function of spinline stress (symbols as in Fig. 5).

Let us consider the values of the birefringence in the two phases Δn_{PS} and Δn_R. If we accept the stress-optical law and uniform stresses for each of the phases, we obtain

$$\Delta n = (1 - \phi)C_{PS}\sigma_{PS} + \phi C_R \sigma_R + \Delta n_{form} \tag{11}$$

The levels of stress are not the same in the two phases. If we were to accept the "elastic" hypotheses of eqs. (4) and (5) or the "viscoelastic" hypotheses of eqs. (6) and (7), we would obtain

$$\Delta n = \left[(1 - \phi)\frac{(1 - \phi)E_{PS}}{\phi E_R + (1 - \phi)E_{PS}} C_{PS} + \phi \frac{E_R}{\phi E_R + (1 - \phi)E_{PS}} C_R\right]\sigma + \Delta n_{form} \tag{12a}$$

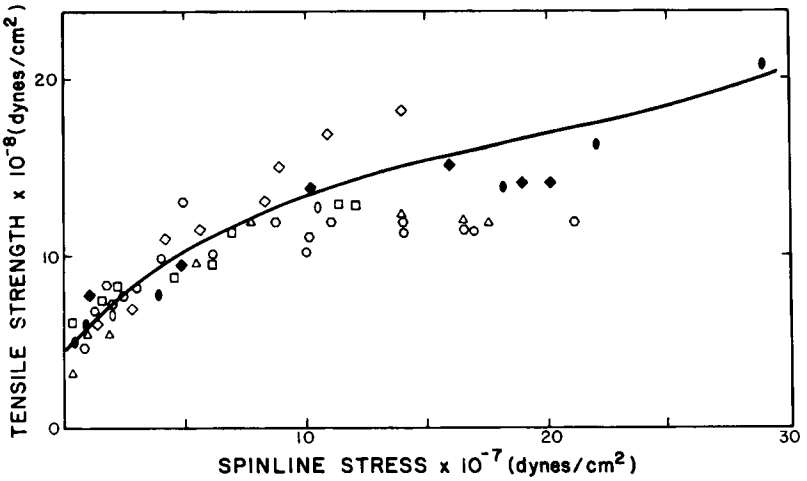

Fig. 9. Tensile strength as a function of spinline stress (symbols as in Fig. 5).

or

$$\Delta n = \left((1-\phi)\frac{(1-\phi)\chi_{PS}}{\phi\chi_R + (1-\phi)\chi_{PS}} C_{PS} + \phi\frac{\phi\chi_R}{\phi\chi_R + (1-\phi)\chi_{PS}} C_R\right)\sigma + \Delta n_{form} \tag{12b}$$

Actually, formulas (12a) and (12b) are oversimplifications and there are stress distributions in each of the phases because of the presences of the particles. The problem of local and global birefringence variations owing to the presence of small rigid particles in a birefringent polymer matrix has been considered in articles by Ong and Stein[34] and Hashiyama and Stein.[35] For small rigid spheres in an elastic matrix, Hashiyama and Stein show that

$$\Delta n = (1-\phi)KC_{PS}\sigma + \phi\Delta n_R + \Delta n_{form} \tag{13a}$$

with

$$K = 1/(1 + (\tfrac{1}{3})\phi) \tag{13b}$$

However, there appear to be no similar solutions for elastic particles.

Let us now apply these results. The value of C_R is 2200,[36] C_{PS} is −4500 B, and ϕ is of order 0.1. If the moduli or elongational viscosities are of the same order of magnitude, we have from eqs. (12),

$$\Delta n \sim C_{PS}\sigma + \Delta n_{form} \tag{14}$$

For a value of ϕ of 0.1, K of eq. (13) is only 0.98, which similarly suggests eq. (14).

Discussion: Form Birefringence

The form birefringence of a suspension of parallel rods in a matrix was derived by Rayleigh[37] and by Bragg and Pippard[38] for a suspension of ellipsoids. These results may be stated as
rods:

$$n_1^2 - n_2^2 = \frac{\phi(1-\phi)(n_R^2 - n_{PS}^2)^2}{(1+\phi)n_{PS}^2 + (1-\phi)^2 n_1^2} \tag{15}$$

ellipsoids:

$$n_1^2 - n_2^2 = \phi(n_R^2 - n_{PS}^2)\,[9K/(3+K)^2](L_2 - L_1)$$

where

$$K = (1-\phi)n_R^2/(n_{PS}^2 - 1) \tag{16}$$

and L_1 and L_2 are the lengths of the major and minor axes of the ellipsoid.

These equations suggest that the form birefringence is positive. Clearly, if our filaments have negative birefringence, the birefringence is not dominated by form birefringence.

We may calculate the levels of Δn_{form} from eqs. (14) and (15). For the cylindrical rod approximations Δn_{form} is of order 10^{-4}, while for the better ellipsoid approximation, it is of order 0.01 to 0.6×10^{-4}. Our measured values range from 10 to 100×10^{-4}. It would appear that form birefringence makes only a very minor contribution. This should be contrasted to the work of Folkes and Kel-

ler,[39] where the opposite conclusion is reached for an extruded filament of a styrene–butadiene SBS block copolymer.

Discussion: Orientation Factors

Having decided the birefringences is due solely to the polystyrene matrix, we may estimate the Hermans orientation factor[15,27–34,41]

$$f = \Delta n/\Delta^0 = (3\langle\cos^2\theta\rangle - 1)/2 \tag{17}$$

where Δ^0 is the intrinsic birefringence. Our values of Δn are in the same range of Oda et al.[15] and those published by other investigators. Accepting Gurnee's value of -0.3 for Δ^0 leads to Hermans orientation factors generally below 0.1 through values as high as 0.13 which were obtained on individual samples.

MECHANICAL PROPERTIES

Results

In Figure 7, we plot force–elongation (F-L) curves obtained on a series of oriented HIPS filaments. These are reduced to the form of engineering stress F/A_0—apparent infinitesimal strain $\Delta L/L_0$. Generally, Young's modulus, yield stress, and tensile strength increase with drawdown and spinline stress (Figs. 8 and 9) while elongation to break decreases with increasing spinline stress (Fig. 10).

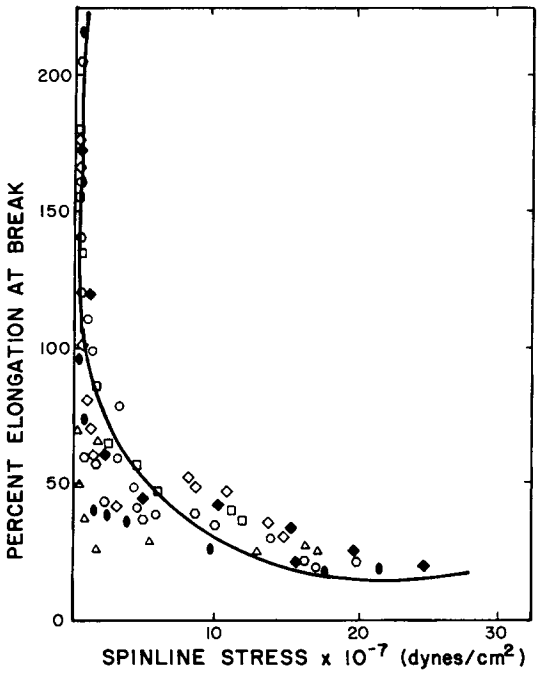

Fig. 10. Elongation to break as a function of spinline stress (symbols as in Fig. 5).

Discussion

Three factors must be considered as possible influences on the mechanical properties of the melt-spun HIPS fibers. These are the orientation of the polystyrene matrix, the rubber morphology, and thermal stresses. Since the effects observed parallel those found in glassy polystyrene[16,17] and in polyolefins[27,28,30] and polyamides,[29,31] it would certainly seem that orientation is important. The properties of the HIPS fibers certainly differ from pure polystyrene.[17] Thus certainly the rubber morphology is important. However, it is not immediately clear that its change with spinning conditions is significant. Thermal stresses are perhaps not as important.

We may also correlate property changes for each individual HIPS with birefringence. An increase in modulus, tensile strength, and yield stress is obtained as birefringence increases. In other experiments in this study[42] it was shown that acrylate rubber-modified polystyrenes show the same trend, but the effect is not as pronounced as in the case of HIPS samples. This would argue that rubber type is significant to property values when the processing stress is changed.

Birefringence-versus-elongation to break results in this study bear an interesting comparison to those reported by Tanabe and Kanetsuna[17] on melt-spun polystyrene filaments. Tanabe and Kanetsuna report a brittle-to-ductile transition at low values of birefringence. The elongation goes rapidly to a maximum and decreases at higher birefringences values. In this study, we only see a comparable decrease in ductility as birefringence increases. Presumably the presence of rubber particles prohibits the system from ever being truly brittle.

The rubber-phase morphology changes are of interest to the mechanical behavior. We concluded above that the spinline stress exceeds the fracture stress of the rubber particles at the process temperature. Thus, the benefit of increased ductility usually associated with rubber reinforced plastics cannot perhaps be entirely maintained when high stresses occur in the process step.

This research was supported in part by the Polymer Section of the National Science Foundation under NSF Grant No. DMR 78-07537 and by the Plastics Institute of America.

References

1. J. Bailey, *Indian Rubber World,* **118,** 225 (1948).
2. R. S. Spencer and G. D. Gilmore, *Mod. Plast.,* **27,** 97 (1950).
3. K. J. Cleereman, H. Karam, and Williams, *Mod. Plast.,* **30,** 125 (1953).
4. R. D. Andrews, *J. Appl. Phys.,* **25,** 1223 (1954).
5. E. F. Gurnee, *J. Appl. Phys.,* **25,** 1232 (1954).
6. E. F. Gurnee, L. T. Patterson, and R. D. Andrews, *J. Appl. Phys.,* **26,** 1106 (1955).
7. J. F. Rudd and R. D. Andrews, *J. Appl. Phys.,* **27,** 996 (1956).
8. R. D. Andrews and J. F. Rudd, *J. Appl. Phys.,* **28,** 1091 (1957).
9. R. L. Ballman and H. L. Toor, *Mod. Plast.,* **37,** 43 (1967).
10. K. J. Cleereman, *SPE J.,* **23,** 43 (1967).
11. L. S. Thomas and K. J. Cleereman, *SPE J.,* **28,** 81 (1972).
12. J. L. S. Wales, I. J. van Leeuwen, and R. van der Vijh, *Polym. Eng. Sci.,* **12,** 358 (1972).
13. M. Fleissner, *Kunststoffe,* **63,** 597 (1973).
14. T. T. Jones, *Pure Appl. Chem.,* **45,** 39 (1976).
15. K. Oda, J. L. White, and E. S. Clark, *Polym. Eng. Sci.,* **18,** 53 (1978).
16. Y. Tanabe and H. Kanetsuna, *J. Appl. Polym. Sci.,* **22,** 1619 (1978).
17. H. Kanetsuna and Y. Tanabe, *J. Appl. Polym. Sci.,* **22,** 2707 (1978).

18. K. Matsumoto and H. Ito, *Sen i Gakkaishi*, **35,** 7–150 (1979).
19. J. L. White and W. Dietz, *Polym. Eng. Sci.*, **19,** 1081 (1979).
20. L. S. Thomas and K. J. Cleereman, *SPE J.*, **28,** 39 (1972).
21. M. R. Grancio, *Polym. Eng. Sci.*, **12,** 213 (1972).
22. M. R. Grancio, A. A. Bibeau, and G. C. Claver, *Polym. Eng. Sci.*, **12,** 450 (1972).
23. R. C. Thamm, *Rubber Chem. Technol.*, **50,** 24 (1967).
24. E. Benaim, J. E. Spruiell, and J. L. White, unpublished research, 1975–1978.
25. J. F. Fellers and B. Kee, *J. Appl. Polym. Sci.*, **18,** 2355 (1974); and J. F. Fellers and D. C. Huang, *J. Appl. Polym. Sci.*, **23,** 2315 (1979).
26. J. F. Fellers and T. F. Chapman, *J. Appl. Polym. Sci.*, **22,** 1029 (1978).
27. J. E. Spruiell and J. L. White, *Polym. Eng. Sci.*, **15,** 660 (1975).
28. J. E. Spruiell and J. L. White, *J. App. Polym. Sci. Appl. Polym. Symp.*, **27,** 121 (1975).
29. V. G. Bankar, J. E. Spruiell, and J. L. White, *J. Appl. Polym. Sci.*, **21,** 2341 (1977).
30. H. P. Nadella, H. M. Henson, J. E. Spruiell, and J. L. White, *J. Appl. Polym. Sci.*, **21,** 3003 (1977).
31. M. D. Danford, J. E. Spruiell, and J. L. White, *J. Appl. Polym. Sci.*, **22,** 3351 (1978).
32. J. L. White and J. E. Spruiell, *J. Appl. Polym. Sci. Appl. Polym. Symp.*, **33,** 91 (1978).
33. R. S. Stein, *Rubber Chem. Technol.*, **49,** 458 (1976).
34. C. S. M. Ong and R. S. Stein, *J. Polym. Sci. Polym. Phys. Ed.*, **12,** 1899 (1974).
35. M. Hashiyama and R. S. Stein, *J. Polym. Sci. Polym. Phys. Ed.*, **16,** 29 (1978).
36. J. Furukawa, T. Kotani, and S. Yamashita, *J. Appl. Polym. Sci.*, **13,** 2541 (1969).
37. Lord Rayleigh, *Philos. Mag.*, **34**(5), 481 (1892).
38. W. L. Bragg and A. B. Pippard, *Acta Crystallogr.*, **8,** 865 (1953).
39. M. J. Folkes and A. Keller, *Polymer*, **12,** 222 (1971).
40. P. H. Hermans and P. Platzek, *Kolloid Z. Z. Polym.*, **88,** 68 (1939).
41. J. J. Hermans, P. H. Hermans, D. Vermaas, and A. Weidinger, *Rec. Trav. Chim.*, **65,** 427 (1946).
42. M. A. A. Omotoso, M.S. thesis, Polymer Engineering, University of Tennessee, Knoxville, 1979.

Received October 4, 1979
Revised January 2, 1980